Migration of low molecular weight components from polymers: 1. Methodology and diffusion of straight-chain octadecane in polyolefins

Shu-Sing Chang
Polymer Science and Standards Division, National Bureau of Standards, Washington, DC 20234, USA
(Received 29 April 1983)

The migration kinetics of monomers, oligomers and antioxidants from several polymers into various solvents at different temperatures has been studied by radioactive tracer techniques. This paper describes in detail the methodology used for observing the migration and for reducing the data. Examples of the migration that follows strictly the Fickian diffusion behaviour with a constant diffusion coefficient are shown. These examples were obtained by first saturating the polyolefin test plaques with a labelled oligomer and then extracting the labelled species from the polymer with identical, but unlabelled, oligomer as the solvent. The polyolefin test plaques were made from linear and branched polyethylene, as well as from isotactic polypropylene. The migrating oligomer was straight-chain octadecane. The diffusion coefficients observed range from 2 to 5 $\mu m^2 s^{-1}$ at 30°C and 7–22 $\mu m^2 s^{-1}$ at 60°C. The activation energies range from 35 to 53 kJ mol^{-1} for the three polymers.

Keywords Alkanes; diffusion; migration; oligomers; polyolefins; radioactive tracer

INTRODUCTION

A large fraction of the polymers produced is used as food packaging materials. Polymeric food packaging materials are essential in modern life to preserve and to aid the distribution of food. In recent years, $\simeq 2$ Tg or four billion pounds of polymer were used for food packing purposes in the US alone[1]. Thus the per capita consumption is approximately 10 kg annually. Approximately two-thirds of these materials are made of polyolefins, i.e., high- and low-density polyethylenes, and polypropylenes. Therefore, it is important to know the amount of any fraction of these food-contacting polymers or their processing additives which migrate into food during packaging, storage and use. The migration levels combined with consumption factors are used together to calculate an estimated daily intake level which would be taken into consideration to determine the safe concentration level of the particular indirect or unintentional food additive in the polymer[2]. A comprehensive study involving many solvents will also be utilized to classify the solvents into different categories, such as simulating or accelerating solvents for oils or fats. The study of the loss of plasticizers and other processing additives may aid the prediction of the service-life for the intended end-use of the plastics incorporating such additives.

Diffusion of low molecular weight substances in and out of a polymer in the presence of a solvent is a complex phenomenon. In general, the diffusion is considered to occur mainly in the amorphous phase. The mechanism changes character for the polymer in the glassy state below the glass transformation region or in the rubbery state above the glass transformation region. Certain cases of the diffusion in the glassy state have been described by a so-called Case II behaviour[3], in which diffusion is rapid in comparison with the slow relaxation process of the polymer network in the glassy state. In the rubbery state, the diffusion phenomenon is generally Fickian. However, the strict adherence to the Fickian behaviour with a constant diffusion coefficient may only be observed in some special cases of migration as that described in this paper. In general, the diffusion of the solvent into the polymer or the swelling of the polymer by the solvent causes the diffusion coefficient of the migrant in the polymer to increase with time.

In this series of papers, a comprehensive data base is presented to aid the modelling of the migration phenomena of low molecular weight species, in various types of polymers and copolymers into or from various types of solvents. The migrants include monomers, oligomers, and processing additives (plasticizers, antioxidants, stabilizers, etc.). The polymers have either amorphous or semicrystalline compositions and are in either rubbery or glassy states. The temperature range of study is from room temperature to 60°C.

In this paper, the detailed experimental protocol for using radioactive tracer techniques for the study of migration kinetics and methods of estimation of diffusion coefficients and partition coefficients is described for this and subsequent papers in this series. Examples are shown for special cases where the Fickian behaviour with a constant diffusion coefficient are strictly obeyed. Parts of this series have been issued in several reports, *cf.* ref. (4), where deviations from a normal Fickian behaviour are more commonly observed.

0032-3861/84/020209-09$03.00

EXPERIMENTAL

Liquid scintillation counting

A liquid scintillation technique was used to monitor the level of radioactivity of ^{14}C. This method is capable of detecting relatively low levels of radioactivity of the order of a few pCi (pico-Curies) with the background counts being of the order of 20–30 counts per minute (c.p.m.) depending on the type of solvent and vial used. This method is also free from effects of sample geometry. However, the radioactive material must be soluble or dispersed in a counting cocktail or in a solvent compatible with the counting cocktail. This method is a destructive test; therefore, the test material is not readily recoverable from the counting solution.

In the determination of radioactivity from counts to disintegration per unit time, e.g., in number of disintegrations per minute (d.p.m.) from the observed counts per minute (c.p.m.), the so-called H-number method[5] of locating the upper edge of the pulse height distribution for the Compton electrons, generated in the counting solution by an external radioactive ^{137}Cs source, was used as the measure of the degree of quenching. This method provides a universal calibration curve of the counting efficiency *versus* the degree of quenching over a very wide range of quenching conditions. The counting efficiency is defined as the observed counts per unit time divided by the radioactivity expressed in disintegrations per unit time.

At low counts, the precision is limited by the statistical error for a Poisson distribution, or the standard deviation $\sigma = N^{1/2}$, where N is the number of counts. The actually observed deviation is often approximately twice that indicated by the Poisson statistics. Samples yielding activities $> 10^6$ c.p.m. should be separated into different vials to avoid gating errors from the counting electronics. At high counts, the precision is limited by the stability of the instrument and most importantly by the reproducibility and precision of the determination of the shift of the Compton edge in the actual sample from an unquenched counting solution. The shift is expressed by an integer H-number from 0 to 1000 which covers logarithmically the energy level up to 2 MeV. With extensive testing, the ultimate precision with which d.p.m. is derived from the counter operated in this mode is of the order of 0.2%, even when the total counts are $\geqslant 10^6$. Therefore, a limit of $2\sigma = 0.2\%$ (10^6 counts) was generally used for samples of high activities, or 10 min counting time for samples of low activities, to terminate the counting process for routine work. A collection of repeated counts to increase the reliability of the results is recorded on magnetic tape and then processed by a large central computer.

Calibration of liquid scintillation counter

The calibration results of a microprocessor-controlled liquid scintillation counter from a commercial unquenched standard of 31 k d.p.m. at 96% efficiency and a commercial standard quenched set of 190 k d.p.m. at 67–96% efficiency are shown in *Figure 1*. These standards are sealed in glass vials and the quenched ones contain CCl_4 as the quenching agent. All these commercial standards are traceable to within 3% of the values of a National Bureau of Standards—Standard Reference Material (NBS-SRM), Carbon-14 (sodium carbonate), that is certified to an accuracy of 1%.

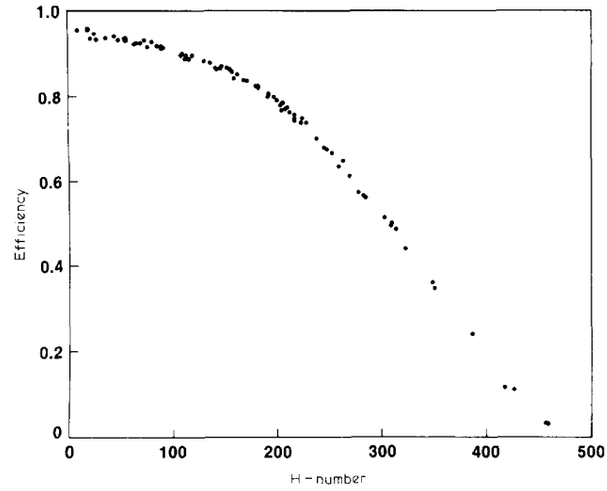

Figure 1 Calibration curve of liquid scintillation counter

The results of calibrating the liquid scintillation counter by NBS-SRM 4222, Carbon-14 (hexadecane), in various commercial counting cocktails* (e.g., EP, GP, HP, NA, OCS, etc.) and with ethanol as the quenching agent are also shown in *Figure 1*. Detailed data are listed elsewhere[6]. Fourteen samples from SRM 4222 were weighed from 0.02 to 0.1 g. The certified specific activity is $3.93_2 \times 10^4$ ($\pm 3\%$) d.p.s. g^{-1}. To each of the samples, known amounts of a counting cocktail and quenching agent, ethanol, were alternatively added to change the quenching levels between an efficiency of 3 and 95% and then counted. The liquid volume in the counting vials varied from 0.5 to 20 ml. From separate experiments it has been established that the liquid volume in the counting vial, varying from 1 to 20 ml, does not affect the counting efficiency beyond the precision of the counting process of $\approx 0.2\%$.

It is clear from the composite graph, *Figure 1*, that regardless of the types of counting cocktails, ^{14}C sources, liquid volumes in the counting vial and quenching agents used, the calibration curve for non-aqueous sample is universal with a precision of $\approx 1\%$ in counting efficiency. The precision is well within the accuracy quoted or certified by the various standards.

For aqueous samples, as long as the liquid in the counting vial remains in a single phase, this observed calibration curve may still be used. When there is a phase separation, the determination of a single H-number to represent both phases becomes uncertain.

Through four years of operation and several repairs, replacements of parts and readjustments of the instrument, the original calibration curve changed slightly. The logarithms of the change in the efficiency appear to increase rectilinearly with the H-number. The change in the efficiency is $\simeq 0.1\%$ at H-number of 75, 0.5% at H-number of 175 and 2% at H-number of 250. As most of the measurements were carried out in the low H-number area, the original calibration curve may still be used with confidence without producing any serious error beyond those of the counting statistics.

* Certain commercial materials and equipment are identified in this paper to specify adequately the experimental procedure. This idenfication does not imply the recommendation or endorsement by the National Bureau of Standards, nor does it imply that the material or equipment identified is necessarily the best available for the purpose.

Extraction methods

Two extraction methods were used: (1) continuous extraction into a limited solvent volume and (2) discrete extraction into a simulated infinite solvent volume.

In method (1) an extraction vial of 25 ml volume with a commercially available Teflon valved cap (Pierce Mininert valves SC-24) is used. Both the body and the sliding valve of the vial cap are made of Teflon. A 2.5 mm diam. silicone rubber septum plug is located just above the valve. When the valve is in the open position, the small hole in the valve plunger lines up with the hole in the body. The diameter of the hole is 1 mm. A hypodermic needle may now pierce the diameter of the silicone plug for removing aliquots by a Teflon-tipped syringe. The syringe and the needle may be left attached to the vial during the entire course of the experiment. The 10–15 ml of solvent in the vial will only contact glass walls and Teflon surfaces during normal experimental processes. Only a small area of the silicone rubber, <1 mm diam., may be exposed to the solvent vapour when the Teflon valve is open. The polymer sample was sometimes surrounded by a nichrome or stainless-steel screen to prevent it from sticking to another sample or to the walls and to keep the sample submerged in the solvent, if the sample has lower density than the solvent.

The vials are placed in closely fitted holes in aluminum blocks which are thermostatically controlled at desired experimental temperature. The so-called dry-bath is placed on a platform of a reciprocating shaker with a linear travelling distance of approximately 2 cm and at an oscillating rate of ≈ 200 reciprocations per min. An aliquot is removed by the syringe from time to time, with a schedule linear in logarithm of elapsed time.

The total amount extracted when t-th aliquot is taken, M_t, is the sum of the amount of migrant in the remaining solution and the amounts that were removed in all aliquots:

$$M_t = C_t W_t + \sum_{i=1}^{t} C_i W_{ai}$$

where C, W, and W_a represent the concentration of the migrant in the solution, the weight of the solution, and the weight of the aliquot, respectively. The partition coefficient is estimated as the ratio of the final concentrations in the solvent *versus* that in the polymer at equilibrium.

In method (2), the polymer sample is immersed in ≈ 10 ml of extracting solvent in a typical 20 ml liquid scintillation counting vial. The vial is placed in a temperature-controlled aluminum block on a reciprocating shaker as described for method (1).

At specific times the sample is removed from the solvent, quickly rinsed and then placed in another vial with fresh solvent to repeat the extraction process. The rinse is combined with the solvent of the previous vial. The total amount of migrant extracted from the polymer at t-th extraction is simply the sum of the amounts of the migrant in all extracts:

$$M_t = \sum_{i=1}^{t} M_i$$

Method (1) is able to yield information about the equilibrium partition coefficient at an infinite extraction or equilibrium time. This method requires knowing accurately the weight or volume ratio of aliquot to total solution and accounting for materials lost during the sampling process for material balance purposes. As the extraction time increases, there is only a very small change in the concentration of extracted material in the solution, whereas a certain weighing or weight ratio and counting error may persist. Therefore, the results for method (1) at long times or at high degree of extraction will show considerable scatter, characteristic of the sampling procedure.

Method (2) is much simpler in operation, but simulates a condition of migration into infinite media. It is relatively free from aforementioned experimental difficulties. However, it should only be used for convenience where the migrant is highly soluble in or miscible with the solvent and thus the results of method (1) and method (2) are indistinguishable. It will not yield equilibrium partition information nor correct migration kinetics for cases where the migrant is sparingly soluble in the solvent.

A third method often used in the literature consists of replenishing the amount of solution aliquot removed for testing with the same amount of fresh solvent, to keep the volume of solvent and exposed surface area ratio the same throughout the experiment. This third method is a hybrid of method (1) and method (2), and thus suffers from the same drawbacks as those of method (2). The third method is not used in the measurements here.

To check the mass balance and variations in the migrant concentration of the sample plaques, radioactivity of the residual migrant remaining in the polymeric sample is monitored by dissolving the sample in toluene at high temperatures after the extraction procedure is ended. It is observed that the single crystals or precipitates of polymer in the counting vial do not interfere with the counting efficiency beyond the normal uncertainty of the counting results.

Calculation of diffusion coefficient

One of the widely used general solutions for the Fickian diffusion equations solved for the case of diffusion either to or from a plane sheet of thickness Lor $2l$ and a stirred liquid of finite volume is presented by Crank[3]:

$$M_t/M_\infty = 1 - \sum_{n=1}^{\infty} \frac{2\alpha(1+\alpha)}{1+\alpha+\alpha^2 q_n^2} \exp(q_n^2 T) \qquad (1)$$

where $\alpha = M_{2\infty}/M_{1\infty} = kV_2/V_1$, $k = C_{2\infty}/C_{1\infty}$, $K = 1/k$ and $T = Dt/l^2$. The subscript 1 denotes the source of the migrant from which the migrant diffuses into the medium, 2. The subscript 2 is sometimes understood for M_t and M_∞ for simplicity.

The solution for the non-zero positive roots, q_n, of:

$$\tan q_n = -\alpha q_n$$

is between $n\pi$ when $\alpha = 0$ and $(n-1/2)\pi$ when $\alpha = \infty$. At $\alpha \ll 1$:

$$q_n \sim n/(1+\alpha).$$

For other values of α:

$$q_n \sim [n - \alpha/2(1+\alpha)]\pi$$

may be used as the starting value in a reiterative numerical computation. From this general solution, several simpler solutions for special cases may be devised.

Equation (1) converges rather slowly at small values of T; thus, a sufficient number of terms must be used to avoid premature termination of the computation. At $T \ll 1$, approximately $3^{(-\log_{10} T)}$ terms are required to reach reasonable precision. The following approaches may be used to simplify the computational effort depending on the conditions and ranges of applications.

The diffusion process may be divided into three regions of T:

Region I, $T<0.1$. $M_t/(1+\alpha)M_\infty$ or $M_t/\alpha M_0$ is a function of T/α^2 only. Before the final approach to equilibrium, a limiting master curve of the quantity $M_t/(1+\alpha)M_\infty$ is a function of T/α^2 may be calculated from equation (1) for small values of α, e.g. 0.001. An alternative simplified method of computation for this region only is described later. However, by limiting the computations in the region $0.1>T>0.001$, the number of terms required may be limited to ≈ 5 at $T \approx 0.1$ and ≈ 45 at $T \approx 0.001$ for reasonable accuracy. The values of $M_t/(1+\alpha)M_\infty$ at small α, but at the same T/α^2, are equal to the values calculated for large α. The results of this selective computation deviate from the more rigorous and tedious computations, by $\approx 0.001\%$ at $T \approx 0.1$, and much less than 0.001% at lower T values. For all practical purposes the values calculated for $\alpha = 0.001$ may be considered as the limiting master curve.

Region II, $5>T>0.1$. The system is approaching equilibrium and detailed computation must be carried out for different α values (only 2—6 terms are required for equation (1) in this region). For $\alpha \ll 1$ and $T/\alpha^2 > 10^3$, $M_t/(1+\alpha)M_\infty = 1-\alpha/(\pi T)^{1/2}$ before reaching equilibrium.

Region III, $T>5$. For all practical purposes, equilibrium has been attained with the deviation $\delta = 1 - M_t/M_\infty \leqslant 10^{-T}$. For $\alpha<1$, equilibrium may be attained much earlier.

Two special cases are worth mentioning here:

(A) *Computation for migration into infinite media.* When $\alpha \rightarrow \infty$, M_t/M_∞ approaches a limit for migration into infinite medium or without partitioning ($M_\infty = M_0$), equation (1) can be reduced to a function of T only:

$$M_t/M_\infty = 1 - 2\sum_{n=1}^{\infty} \frac{1}{q_n^2} \exp(-q_n^2 T) \qquad (2)$$

where $q_n = (n-1/2)\pi$. For small T, M_t/M_∞ is proportional to $T^{1/2}$.

$$M_t/M_\infty = 2(T/\pi)^{1/2} = 1.128379\,T^{1/2} \qquad (3)$$

Deviations of equation (3) from equation (2) are less than 10^{-10} at $T<0.5$ ($M_t/M_\infty \approx 0.25$), $\approx 10^6$ at $T=0.1$ ($M_t/M_\infty \approx 0.35$), $\approx 5\times 10^4$ at $T=0.2$ ($M_t/M_\infty \sim 0.5$) and becomes much greater than 0.01 at $T=0.3$ ($M_t/M_\infty \approx 0.6$) or higher.

(B) *Alternate approximation.* An alternative form of the solution[3]:

$$M_t/M_\infty = (1+\alpha)[1-\exp(T/\alpha^2)\,erfc(T^{1/2}/\alpha)] \qquad (4)$$

may be used in some cases and is relatively simple to compute. One of the rational approximations[7] for the error function yields the following:

$$M_t/(1+\alpha)M_\infty = 1 - \sum_{n=1}^{5} a_n \tau^n \qquad (5)$$

where $\tau = 1/(1+0.3275911\,T^{1/2}/\alpha)$, $a_1 = 0.254829592$, $a_2 = -0.28449636$, $a_3 = 1.421413741$, $a_4 = -1.453152027$, $a_5 = 1.061405429$. The quoted error of approximating the error function is $<1.5\times 10^{-7}$. At $\alpha \ll 1$, results computed from equation (5) deviate $<0.01\%$ from that of equation (1) at $T/\alpha^2 < 5$ or at $M_t/(1+\alpha)M_\infty < 0.75$. Equation (5) is not applicable at $T \geqslant 1$ and $\alpha > 100$. It does not yield reliable information in the region approaching equilibrium, nor at larger values of α where infinite bath approach may be used and, hence, should be used with discretion.

By combining equation (3) at $T<0.1$ and $\alpha>100$, equation (5) at small α, $T/\alpha^2<5$ and $T<0.1$ (Region I) and equation (1) at $T>0.1$ (Regions II and III), computational efforts for the solution of the diffusion equation between a plane sheet and a well-stirred liquid may be reduced to a minimum. Numerical values for all three regions and for various conditions are listed elsewhere[8].

The equilibrium partition fixes the fractional amount migrated at infinite time as:

$$\frac{M_\infty}{M_0} = \frac{\alpha}{1+\alpha}$$

The fractional amount left in the source at equilibrium is $M_{1\infty}/M_0 = 1/(1+\alpha)$. As either k or V_2 becomes very large, α becomes very large, and M_∞ approaches M_0. M_0 is equal to (M_1+M_2). However, if the solution concentration is determined by sampling the aliquots, then the total amount of migrant in the aliquots should be added to M_2 for extraction or subtracted from M_0 for absorption.

The following relation may be used to convert the fraction migrated, M_t/M_∞, to amount migrated per unit area of exposure:

$$\frac{M_t}{A} = 2lC_0 \frac{\alpha}{1+\alpha}\frac{M_t}{M_\infty}$$

where A is the area of one side of the plane sheet, l is the half thickness, and C_0 is the original migrant concentration in the sheet.

The fractional amount migrated into the solution from the original migrant content in the polymer sheet, M_t/M_0, is represented in a log–log plot against the reduced time, $T = Dt/l^2$, for various α (as a result from partition coefficient k and the volume ratio) in *Figure 2*. Only in the case where α is very large or the migrant is almost totally extractable, the amount migrated, M_t/M_∞ or M_t/M_0, will be proportional to $t^{1/2}$ up to ≈ 0.6. This rectilinearity is obeyed to a much lower level of M_t/M_∞ at smaller α. For instance, the deviation from a $t^{1/2}$ rectilinearity has already attained a level of $\approx 2.5\%$ at $M_t/M_\infty = 0.4$ for $\alpha = 10$. The deviation at high M_t/M_∞ increases as α decreases. The deviation remains of the order of 8% at $M_t/M_\infty = 0.1$ for $\alpha < 0.1$. Therefore, unless the migrant is totally extractable or the level of migration is limited to $<10\%$ of M_∞ for all cases involving partitioning, it is not advisable to estimate the diffusion coefficient from the initial slope of M_t *versus* $t^{1/2}$ as outlined by equation (3).

For these reasons the results are presented here in a $\log(M_t/M_0)$ *versus* $\log t$ plot instead of the more commonly used rectilinear M_t *versus* $t^{1/2}$ plot. The $t^{1/2}$ plot will allow only one decade of M_t to be shown significantly; however, the log–log plot will allow the

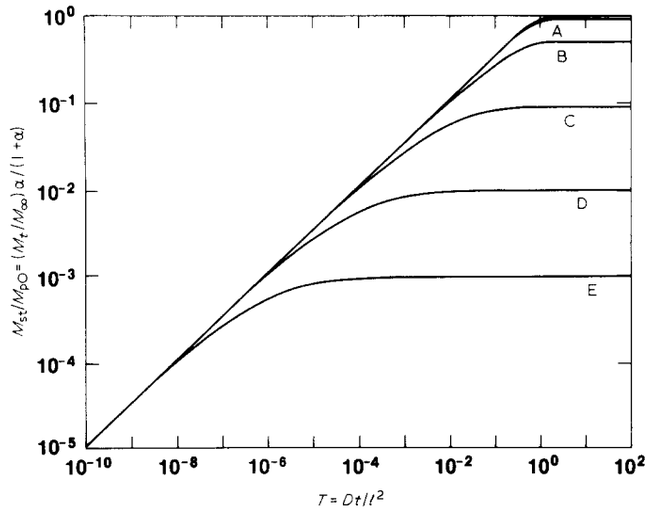

Figure 2 Fractional amount migrated as a function of reduced time, T, at α, A, 10; B, 1; C, 0.1; D, 0.01; E, 0.001

simultaneous showing of many decades of M_t. The only drawback of the log–log plot is the compression of the data near M_∞/M_0. For the present study the detailed kinetics in this region is of relatively low importance, as the amount migrated in this region does not differ significantly from an equilibrium migration.

The diffusion coefficients may be estimated from *Figure 2* by appropriate shifts or calculated by means of regression from equation (1) in general or from equation (3) or (5) when $T<0.1$ in appropriate cases. In the case of increase of D from an initial low value to a higher value, due to solvent swelling, the maximum D at later times is obtained by fitting the final portion of the diffusion curve only. In the case of partitioning, the computation of D is also sensitive to the assignment of α or k.

Materials

The two polyethylene samples were made from the stocks from which two National Bureau of Standards, Standard Reference Materials (NBS-SRM): 1475, linear polyethylene (LPE) whole polymer; and 1476, branched polyethylene (BPE) whole polymer, were characterized[9,10]. The weight- and number-average molecular weights for the LPE or high density polyethylene are 53 000 and 18 300, and those for the BPE or low-density polyethylene are $\approx$100 000 and 24 000, respectively. The polypropylene samples were prepared from a commercial food-packaging grade isotactic polypropylene of weight-average molecular weight 290 000.

The labelled and unlabelled n-$C_{18}H_{38}$ were produced from commercial sources and were believed to be at least 96% pure. The original specific activities of the two batches of ^{14}C-labelled n-$C_{18}H_{38}$ were 13 and 86 mCi g^{-1}, respectively.

Plaques saturated with radioactive n-$C_{18}H_{38}$ were prepared as follows. Raw pellets of linear and branched polyethylene, and polypropylene were press molded into sheets of 0.025–0.07 cm thickness. These sheets were cut into test pieces of suitable sizes. The test pieces were immersed for one month or longer in molten straight-chain octadecane at 30° or 60°C. The liquid straight-chain octadecane was doped with high specific activity n-$C_{18}H_{38}$-1-^{14}C to yield a specific activity of 2.34 μCi g^{-1}. A portion of the low molecular weight distribution of these polymers may be removed by the immersion in straight-chain octadecane. The amount of the low molecular weight portion removed may be similar to that removable by straight-chain heptane[11], of the order of 0.5% from linear polyethylene to $<2\%$ from branched polyethylene.

RESULTS AND DISCUSSION

The polymer plaques were first saturated with radioactive n-$C_{18}H_{38}$. These plaques were then extracted by molten unlabelled n-$C_{18}H_{38}$ in the manner as described for simulated infinite bath, method (2), described previously. As the migrant and the solvent are of the same chemical compound, the migrant is totally compatible and soluble in the solvent; therefore, $M_\infty = M_0$. In the latter cases the results from method (1) using limited solvent volume and method (2) using unlimited solvent volume are indistinguishable. As the polymers were already saturated with n-$C_{18}H_{38}$, no net change in the n-$C_{18}H_{38}$ concentration should occur within the polymer; therefore, no concentration effects (presumably due to the plasticization action of the low molecular weight species) on the diffusion coefficients should be observed. Thus, only the exchange of the labelled species with the unlabelled species of n-$C_{18}H_{38}$ are observed.

When the submerged polymer samples were removed from molten straight-chain octadecane, an amount of octadecane adhered to the surface was not removed prior to the exchange experiment. The first few data points (within the first 1 min of the experiment) contained all of the migrant on the surface and part of the migrant from the interior of the polymer. By rectilinearly extrapolating the amount extracted *versus* $t^{1/2}$ to $t=0$ for the early data points, the extrapolated intercept from a rectilinear line indicates the amount of migrant on the surface. This amount was subtracted from the observed total amount extracted to give the amount migrated from the interior of the polymer alone. The amount adhered to the surface was of the order of 1–2 mg cm^{-2}.

The parameters of these experiments are summarized in *Table 1*. The diffusion coefficient of experiment (3) appears to be lower than generally expected. The n-$C_{18}H_{38}$ content is also the lowest. It is possible that the absorption of n-$C_{18}H_{38}$ has not attained the asymptote thus causing a low diffusion coefficient. The octadecane concentration was estimated from the total activity of the sample divided by the weight of the final sample. The concentration estimated from radioactivity is within 0.5% of the values calculated from the weight gain from the original polymer plaque before the absorption of n-$C_{18}H_{38}$. Unlabelled octadecane adhered on the surface of the final sample was quickly rinsed off with ethanol. The loss of some low molecular weight fractions of the polymer plaques in the n-$C_{18}H_{38}$ bath introduced additional uncertainties to estimates of concentration by weight gains.

Experimental data are presented in *Table 2* and shown in *Figures 3* and *4*. Some numerical data within 0.002 of M_∞ are omitted in the Table for clarity. The curves are represented in a log–log plot with the time scale reduced by thickness effects. The results of experimental no. 6, diffusion of saturated n-$C_{18}H_{38}$ in branched polyethylene at 30°C, are shown in three different representations, *Figure 5*(*a*), (*b*) and (*c*). The solid curves in all the Figures represent the theoretical curve calculated for a

Table 1 Summary of diffusion of n–$C_{18}H_{38}$ in polyolefins

Expt. no.	Polymer	Thickness (cm)	Exposed area (cm^2)	Sample wt. (g)	Specific activity (μCi/g polymer)	$C_{18}H_{38}$ conc. (wt%)	t (°C)	D ($\mu m^2\ s^{-1}$)
1	LPE	0.089	8.3	0.326	0.113	4.8	30	4.5
2	LPE	0.027	3.8	0.045	0.133	5.7	30	4.4
3	LPE	0.085	9.0	0.341	0.103	4.4	60	9.6
4	LPE	0.027	11.7	0.154	0.121	5.2	60	17.0
5	BPE	0.065	3.6	0.099	0.245	10.5	30	3.9
6	BPE	0.066	4.5	0.114	0.220	9.4	30	2.8
7	BPE	0.065	3.7	0.100	0.235	10.0	60	22.0
8	PP	0.028	5.2	0.061	0.165	7.0	30	1.7
9	PP	0.027	6.1	0.071	0.157	6.7	60	6.8

Table 2 A. Diffusion of n–$C_{18}H_{38}$ in linear polyethylene

1. LPE, 0.089 cm, 30°C		2. LPE, 0.027 cm, 30°C		3. LPE, 0.085 cm, 60°C		4. LPE, 0.027 cm, 60°C	
t (h)	M_t/M_0	t (h)	M_t/M_0	t (h)	M_t/M_0	t (h)	M_t/M_0
0.167	0.129	0.012	0.109	0.167	0.169	0.033	0.376
0.333	0.185	0.017	0.128	0.333	0.278	0.083	0.582
0.667	0.264	0.025	0.155	0.667	0.404	0.167	0.772
1	0.319	0.033	0.180	1	0.493	0.333	0.923
2	0.426	0.05	0.219	1.5	0.601	0.667	0.981
4	0.561	0.067	0.254	2.5	0.734	1	0.990
8	0.714	0.083	0.285	4	0.864	1.5	0.992
24	0.940	0.104	0.317	6	0.937	7	0.994
48	0.991	0.133	0.361	8	0.971	199	0.997
79.5	0.997	0.167	0.405	23	0.994		
389	1.000	0.25	0.522	319	0.996		
		0.337	0.599				
		0.504	0.708				
		0.667	0.784				
		1	0.875				
		1.5	0.934				
		2	0.955				
		3	0.968				
		4.5	0.972				
		6	0.975				
		8	0.976				
		25.3	0.981				

B. Diffusion of n–$C_{18}H_{38}$ in branched polyethylene

5. BPE, 0.065 cm, 30°C		6. BPE, 0.066 cm, 30°C		7. BPE, 0.065 cm, 60°C	
t (h)	M_t/M_0	t (h)	M_t/M_0	t (h)	M_t/M_0
0.008	0.0402	0.011	0.0370	0.011	0.104
0.021	0.0587	0.019	0.0466	0.017	0.143
0.033	0.0737	0.025	0.0546	0.025	0.166
0.05	0.0905	0.035	0.0656	0.033	0.198
0.083	0.117	0.053	0.0774	0.05	0.218
0.117	0.140	0.067	0.089	0.067	0.248
0.183	0.176	0.1	0.110	0.1	0.305
0.233	0.197	0.133	0.126	0.133	0.350
0.35	0.240	0.183	0.147	0.167	0.391
0.5	0.279	0.25	0.172	0.25	0.476
0.733	0.345	0.333	0.198	0.333	0.544
0.983	0.400	0.483	0.238	0.5	0.652
1.48	0.484	0.736	0.294	0.75	0.770
1.98	0.550	0.985	0.339	1	0.848
2.98	0.649	1.49	0.415	1.5	0.932
3.98	0.721	1.98	0.477	2	0.969
5.98	0.820	2.98	0.577	3	0.992
8.98	0.904	4.53	0.694	5	0.998
23.8	0.987	5.98	0.771	150	0.999
32	0.991	8.22	0.852		
56	0.993	23.9	0.981		
173	0.995	32.3	0.987		
		100.0	0.991		

C, Diffusion of $n-C_{18}H_{38}$ in polypropylene

8. PP, 0.028 cm, 30°C		9. PP, 0.027 cm, 60°C	
t (h)	M_t/M_0	t (h)	M_t/M_0
0.011	0.0639	0.011	0.124
0.017	0.0785	0.017	0.152
0.025	0.0975	0.025	0.184
0.033	0.114	0.033	0.214
0.05	0.136	0.05	0.261
0.067	0.157	0.067	0.302
0.1	0.188	0.1	0.378
0.133	0.215	0.133	0.444
0.167	0.238	0.167	0.504
0.25	0.289	0.25	0.627
0.333	0.332	0.333	0.718
0.5	0.406	0.5	0.839
0.75	0.499	0.75	0.927
1.02	0.584	1	0.968
1.5	0.701	1.5	0.993
2	0.786	2	0.998
3	0.890	30.9	0.999
4.5	0.959		
6.25	0.987		
8.93	0.997		
30.9	0.999		

diffusion coefficient of 2.8 $\mu m^2 s^{-1}$ or 2.8×10^{-8} $cm^2 s^{-1}$. As mentioned previously, the advantage of the $t^{1/2}$ plot (b) is the rectilinear behaviour at $M_t/M_\infty < 0.6$, if nearly all the migrant is extractable, $M_\infty \approx M_0$. The log–log plot (c) has the advantage that the theoretical curves for different diffusion coefficients retain the same shape with a linear translation in the time axis. The log–log plot also allows the display of many decades of data. Illustrations (a) and (b) are only effective for one decade of M_t, t or $t^{1/2}$. The only disadvantage of the log–log plot (c) is the compression of the data near equilibrium, M_∞.

Almost all the experiments shown in *Figures 3* and *4* appear to follow the Fickian behaviour as calculated by equation (3) for $M_t/M_0 < 0.6$ and by equation (1) for the region approaching equilibrium. In some of the experiments M_∞ may be slightly less than M_0. For experiment no. 9, the enhancement (similar to a swelling effect) at $M_t/M_0 > 0.4$ ($t > 10$ min) is probably an indication that the sample has not yet attained an equilibrium absorption of the migrant. Deviations from the idealized Fickian behaviour are commonly observed in plaques not saturated with swelling agent[4,6,8].

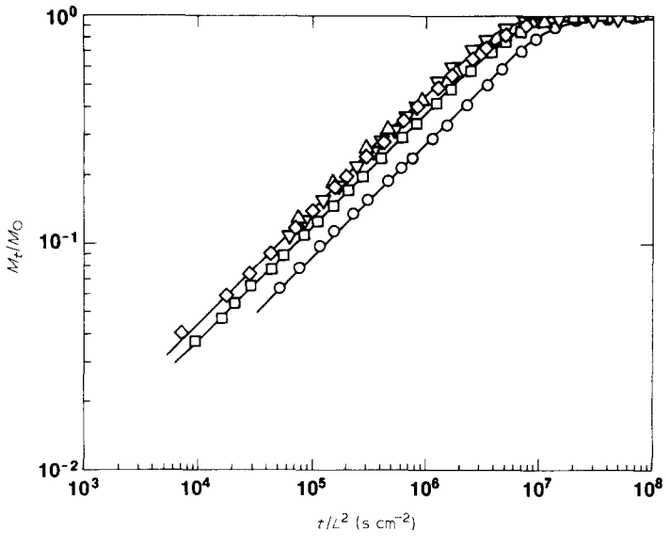

Figure 3 Diffusion of n-$C_{18}H_{38}$ in Polyolefins at 30°C. LPE: △, Expt. no. 1; ▽, Expt. no. 2. BPE: ◇, Expt. no. 5; □, Expt. no. 6. PP: ○, Expt. no. 8

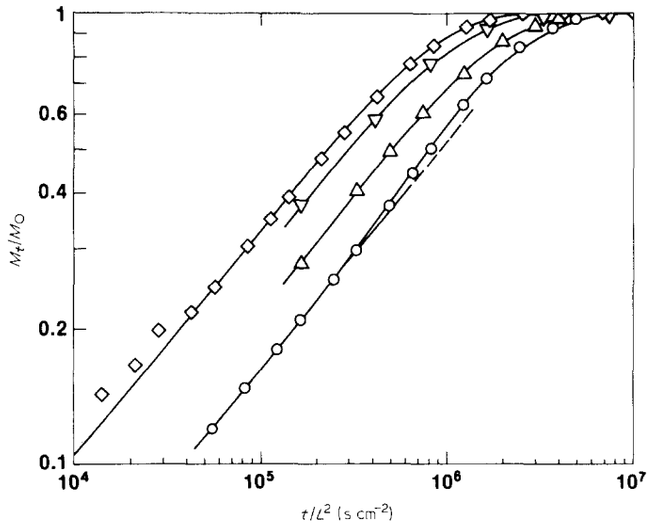

Figure 4 Diffusion of n-$C_{18}H_{38}$ in polyolefins at 60°C. LPE: △, Expt. no. 3; ▽, Expt. no. 4. BPE: ◇, Expt. no. 7. PP: ○, Expt. no. 9

By assuming that the absorption of octadecane occurs only in the amorphous phase but not in the crystalline lattice and that the nominal amorphous fractions for the linear and branched polyethylene are 0.25 and 0.45, respectively, the maximum uptake of octadecane of 5 wt% by LPE and 10 wt% by BPE indicates that the absorption of octadecane is ≈20% in the amorphous phase of either polyethylenes. As the diffusion coefficients are similar in both polyethylenes, apparently the presence of the

crystalline phase does not affect significantly the diffusion of octadecane in the equilibrium swollen amorphous phase.

The diffusion coefficients are 4 and 20 $\mu m^2 s^{-1}$ based on the whole polymer at 30° and 60°C, respectively, for either of the polymers saturated with octadecane. These diffusion coefficients are much smaller than the self-diffusion coefficients of 310 and 550 $\mu m^2\ s^{-1}$ [12] for

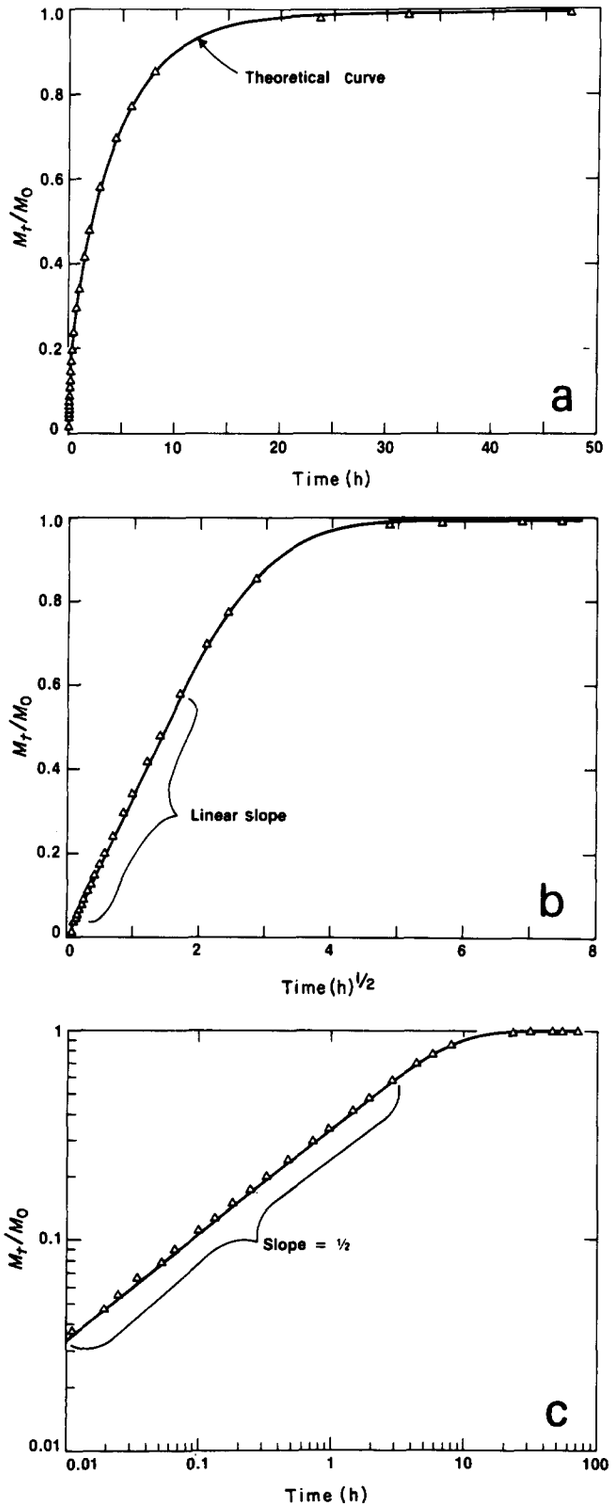

Figure 5 (a), (b), and (c). Diffusion of n-$C_{18}H_{38}$ in branched polyethylene at 30°C (Expt. no. 6)

octadecane at corresponding temperatures. The diffusion coefficients observed for the diffusion of n-$C_{18}H_{38}$ from saturated branched polyethylene are slightly higher than that observed for the diffusion of n-$C_{18}H_{38}$ between two sheets of low-density polyethylene intimately in contact with each other[13]. On the average the values here are ≈ 1.5 times larger than those in ref. 13. This difference is probably the result of the concentration dependence of the diffusion coefficients. The initial concentration of n-$C_{18}H_{38}$ in the studies of Auerbach *et al.*[13] was 1.3–1.5%, whereas the concentrations of n-$C_{18}H_{38}$ in the studies here for the branched polyethylene remained constant during the experiment at 9–10%.

For the narrow temperature region studied, in the absence of any transitions, the diffusion coefficient may be interpolated by a simple Arrhenius equation:

$$D = D_0 \exp(-E/RT) \quad (4)$$

with an apparent activation energy, E, of 53 kJ mol^{-1} for the diffusion of n-$C_{18}H_{28}$ from branched polyethylene which is nearly the same as 51 kJ mol^{-1} as estimated in ref. 13. The activation energies for the migration of n-$C_{18}H_{38}$ from linear polyethylene and isotactic polypropylene from the studies here are estimated to be 35 and 39 kJ mol^{-1}, respectively.

The diffusion coefficients of octadecane in polypropylene saturated with octadecane is ≈ 2 to 3 times less than that in polyethylene at the same temperature. The presence of a methyl group at every other chain element may increase the tortuousity or the impedance of the movement of the diffusant.

The final polymeric sample was dissolved in hot toluene to measure any residual activities still remaining in the polymer. Except for the two 30°C experiments, all other exchanges were at least 99.5% complete. These two samples, with M_∞/M_0 of 98–99% at the equilibrium extraction, had been left in the molten octadecane for 18 months. Therefore, some exchange or incorporation of the radioactive octadecane molecules may have occurred with the crystalline phase. The diffusion in the crystalline phase will be many orders of magnitude slower than that in the amorphous phase for temperatures above the glass transformation region. It is noteworthy that residual activities in the polymer should also be determined, not only to establish the uniformity of migrant distribution in different test pieces but also to serve as an indicator for any deviation in the actual migrant content from the original composition of the polymer–migrant mixture. This is especially important in cases where the migrant may be volatile in highly disperse conditions as examined in the later papers of this series. The actual amounts of migrant in the solvent and in the polymer are parameters in determining the total activities and the partition coefficients; thus, neither should be assumed from the gross original composition. Portions of the migrant not available for ready migration for any reason should also be accounted for properly.

CONCLUSIONS

The diffusion of n-$C_{18}H_{38}$ in polyethylene, with no net change in the concentration of n-$C_{18}H_{38}$ except in the isotopic composition, is shown here to obey the ideal Fickian diffusion laws.

In subsequent papers of this series, the phenomena of the migration of straight-chain alkanes from polyolefins, the migration of BHT (2,6-di-*t*-butyl-4-hydroxytoluene) from various polymers, and the migration of styrene monomer from polystyrene, into various solvents will be examined. In most of these cases, deviations from idealized Fickian behaviour are observed.

ACKNOWLEDGEMENT

The author wishes to thank Bert M. Coursey for discussions in radioactivity counting, and Walter J. Pummer and John R. Maurey for co-operation in sample preparations and measurements.

REFERENCES

1 Diernisse, V. 'Plastics in Food Packaging', Business Communications Co., Stamford, CT 1980
2 *Food Chem. News* 1982, **23**, (52) 34
3 Crank, J. 'The Mathematics of Diffusion' Clarendon Press, Oxford, 1975
4 Chang, S. S., Senich, G. A. and Smith, L. E. NBSIR 822472, US Nat. Bur. Stand., 1982. Available as NTIS PB82-196403
5 Horrocks, D. L. 'The H-number Concept', Tech. Rept. 1095-NUC-77-IT, Beckmann Instrum. Inc., Fullerton, CA, 1972
6 Smith, L. E., Sanchez, I. C. Chang, S. S. NBSIR 79-1598, US Nat. Bur. Stand., 1969. Available as NTIS PB-297671
7 Abramowitz, M. and Stegun, I. A. 'Handbook of Mathematical Functions', Nat. Bur. Stand. Appl. Math. Ser. 55, 1972, ch. 7, p. 297
8 Smith, L. E., Chang, S. S., McCrackin, F. L., Senich, G. A. and Wang, F. W. NBSIR 81-2264, US Nat. Bur. Stand., 1981. Available as NTIS PB 81-202749
9 Wagner, H. L. and Verdier, P. H. (Eds.) NBS SP 26042, US Nat. Bur. Stand., 1972
10 Wagner, H. L. and McCrackin, F. L. *J. Appl. Polym. Sci.* 1977, **21**, 2833
11 Chang, S. S., Pummer, W. J. and Maurey, J. R. *Polymer* 1983, **24**, 1267
12 Douglass, D. C. and McCall, D. W. *J. Phys. Chem.* 1958, **62**, 1102
13 Auerbach, I., Miller, W. R., Kuryla, W. C. and Gehman, S. D. *J. Polym. Sci.* 1958, **28**, 129